Molecules and Cells

Biphasic Regulation of Mitogen-Activated Protein Kinase Phosphatase 3 in Hypoxic Colon Cancer Cells

Hong Seok Kim[1,*], Yun Hee Kang[2,3], Jisu Lee[3], Seung Ro Han[2,3], Da Bin Kim[1,4], Haeun Ko[5], Seyoun Park[5], and Myung-Shin Lee[3,*]

[1]Department of Molecular Medicine, College of Medicine, Inha University, Incheon 22212, Korea, [2]Eulji Biomedical Science Research Institute, Eulji University School of Medicine, Daejeon 34824, Korea, [3]Department of Microbiology and Immunology, Eulji University School of Medicine, Daejeon 34824, Korea, [4]Program in Biomedical Science and Engineering, College of Medicine, Inha University, Incheon 22212, Korea, [5]Medical Course, College of Medicine, Inha University, Incheon 22212, Korea
*Correspondence: kimhs0622@inha.ac.kr (HSK); imslee@gmail.com (MSL)
https://doi.org/10.14348/molcells.2021.0093
www.molcells.org

Hypoxia, or low oxygen tension, is a hallmark of the tumor microenvironment. The hypoxia-inducible factor-1α (HIF-1α) subunit plays a critical role in the adaptive cellular response of hypoxic tumor cells to low oxygen tension by activating gene-expression programs that control cancer cell metabolism, angiogenesis, and therapy resistance. Phosphorylation is involved in the stabilization and regulation of HIF-1α transcriptional activity. HIF-1α is activated by several factors, including the mitogen-activated protein kinase (MAPK) superfamily. MAPK phosphatase 3 (MKP-3) is a cytoplasmic dual-specificity phosphatase specific for extracellular signal-regulated kinase 1/2 (Erk1/2). Recent evidence indicates that hypoxia increases the endogenous levels of both MKP-3 mRNA and protein. However, its role in the response of cells to hypoxia is poorly understood. Herein, we demonstrated that small-interfering RNA (siRNA)-mediated knockdown of MKP-3 enhanced HIF-1α (not HIF-2α) levels. Conversely, MKP-3 overexpression suppressed HIF-1α (not HIF-2α) levels, as well as the expression levels of hypoxia-responsive genes (*LDHA*, *CA9*, *GLUT-1*, and *VEGF*), in hypoxic colon cancer cells. These findings indicated that MKP-3, induced by HIF-1α in hypoxia, negatively regulates HIF-1α protein levels and hypoxia-responsive genes. However, we also found that long-term hypoxia (>12 h) induced proteasomal degradation of MKP-3 in a lactic acid-dependent manner. Taken together, MKP-3 expression is modulated by the hypoxic conditions prevailing in colon cancer, and plays a role in cellular adaptation to tumor hypoxia and tumor progression. Thus, MKP-3 may serve as a potential therapeutic target for colon cancer treatment.

Keywords: colon cancer, hypoxia, hypoxia-inducible factor-1α, mitogen-activated protein kinase phosphatase 3

INTRODUCTION

Hypoxia is a common characteristic of solid malignant tumors (Harris, 2002). Since oxygen can only diffuse to approximately 100-200 μm away from a capillary (Olive et al., 1992), tumor cells encounter hypoxic stress at a very early stage during cancer development. While reduced oxygen tension can be lethal for certain cells, several tumor cells are able to survive under hypoxic conditions. It is well established that hypoxia plays a critical role in every aspect of cancer biology, including cell immortalization and stem cell maintenance, genetic instability, glucose and energy metabolism, vascularization, autocrine growth factor signaling, invasion and metastasis, immune evasion, and resistance to chemotherapy and radiation therapy through HIF-1 induction (Byun et al., 2020;

Received 7 April, 2021; revised 20 August, 2021; accepted 20 August, 2021; published online 20 October, 2021

eISSN: 0219-1032

Harris, 2002; Semenza, 2010). Thus, hypoxia is a significant impediment to successful cancer therapy.

The hypoxia-inducible factor (HIF) pathway is required for the adaptive response of tumor cells to hypoxia (Semenza, 2012). HIF is a heterodimeric transcription factor consisting of an oxygen-regulated α subunit (HIF-1α, HIF-2α, or HIF-3α) and a constitutively expressed β subunit (HIF-1β; Rankin and Giaccia, 2008). In the HIF-α family, the function and activity profile of HIF-1α is the most well evaluated; furthermore, the clinical application of HIF-1α has been proposed as a promising strategy for the development of new therapies for cancer. Overall, HIF-1α activity is regulated mainly through post-translational modification and stabilization of the HIF-1α subunit. In hypoxic environments, HIF-1α accumulates because of impaired degradation (mediated via its hydroxylation and proteasomal degradation). HIF-1α then heterodimerizes with HIF-1β and translocates into the nucleus to initiate its transcriptional program (Wenger et al., 2005). Although proline hydroxylation and VHL-mediated degradation are well-established mechanisms involved in HIF-1α stability, phosphorylation induced by mitogen-activated protein kinase (MAPK) can also influence its stability, nuclear localization, and transcriptional activity in various types of cancer cells (Kietzmann et al., 2016; Wagner and Nebreda, 2009).

MAPKs are widely expressed Ser/Thr kinases that are involved in the regulation of a wide array of cellular processes, such as cell proliferation, differentiation, metabolism, motility, survival, and apoptosis (Chang and Karin, 2001). The three major MAPK subfamilies, including the extracellular signal-regulated kinases (Erk1/2), p38, and Jun N-terminal kinase (JNK), play crucial roles in the development and progression of cancer, including colon cancer (Dhillon et al., 2007; Urosevic et al., 2014; Zhu et al., 2012).

The activity of MAPKs is tightly regulated by Ser/Thr-, dual-specificity-, and Tyr-specific phosphatases (Keyse, 2000). However, the primary group of phosphatases that dephosphorylate both tyrosine and threonine residues of the signature T-X-Y motif located within the activation loop of the MAPKs is the MAPK phosphatase (MKP) family, which serve as endogenous negative regulators of MAPKs (Caunt and Keyse, 2013). MKPs belong to a dual-specificity phosphatase (DUSP) family, and the ten catalytically active MKPs can be grouped according to sequence homology, subcellular localization, and substrate specificity. MKP-1 (DUSP1), PAC-1 (DUSP2), MKP-2 (DUSP4), and hVH3 (DUSP5) are mitogen- and stress-inducible nuclear MKPs. MKP-3 (DUSP6), MKP-4 (DUSP9), and MKP-X (DUSP7) are cytoplasmic ERK-specific MKPs. MKP-5 (DUSP10), MKP-7 (DUSP16), and hVH5 (DUSP8) are JNK/p38–specific phosphatases, which are found in both the nucleus and cytoplasm (Camps et al., 2000). As MKPs negatively regulate MAPKs, a tumor-suppressor role for MKPs has also been proposed in several cancers (Furukawa et al., 2003; Shen et al., 2019; Waha et al., 2010). In contrast, the gain of MKP expression has also been associated with cancer progression, drug resistance, and poor patient prognosis (Keyse, 2008). Due to the emerging role of MKPs in regulating cancer cell growth and death, an increasing number of studies have focused on the role of MKPs in cancer. However, despite this increased emphasis, the role of MKPs in tumor hypoxia remains poorly defined.

In the current study, we focused on the changes in the expression and function of MKP-3 in hypoxic colon cancer cells. Our results demonstrated that short-term hypoxia-induced MKP-3 negatively regulates HIF-1α protein levels but not HIF-2α levels. Interestingly, long-term hypoxia, a hallmark of the inner core of numerous solid tumors, induces the lactic acid-mediated proteasomal degradation of MKP-3. We further showed that the loss of MKP-3 in colon cancer cells promotes proliferative and migratory phenotypes.

MATERIALS AND METHODS

Reagents

N-acetyl-L-cysteine (NAC; A9165), MG132 (474790), lactic acid (252476), actinomycin D (A9415), and sodium oxamate (O2751) were purchased from Sigma-Aldrich (USA). The MAPK inhibitors PD98059 (S1177), SB203580 (S1076), and SP600125 (S1460) were purchased from Selleck Chemicals (USA). The fluorogenic probe, 2′, 7′-dichlorodihydrofluorescein diacetate (H2DCFDA; D399) was obtained from Thermo Fisher Scientific (USA). Primary antibodies against p-ERK1/2-Thr202/Tyr204 (#4370), ERK1/2 (#9102), β-actin (#3700), and LDHA (#2012) were purchased from Cell Signaling Technology (USA). Antibodies against HIF-1α (MAB1536), HIF-2α (NB100-122), MKP-3 (ab76310), and ubiquitin (ab134953) were obtained from R&D Systems (USA), Novus Biologicals (USA), and Abcam (UK), respectively. Secondary antibodies, including anti-mouse HRP-linked IgG antibody (sc-516102) and anti-rabbit HRP-linked IgG antibody (sc-2357), were obtained from Santa Cruz Biotechnology (USA).

Cell culture

Three human colon cancer cell lines (RKO, DLD-1, and HCT 116) and murine CT26 colon cancer cells were obtained from the American Type Culture Collection (ATCC) and cultured in Dulbecco's modified Eagle's medium (DMEM) (HyClone Laboratories, USA) supplemented with 10% fetal bovine serum (HyClone Laboratories) and 1% antibiotic–antimycotic (Thermo Fisher Scientific). All cell lines were cultured at 37°C under a humidified atmosphere containing 5% CO_2. Hypoxic conditions (0.5% O_2) were achieved by placing the cells in an InvivO2 500 hypoxia workstation (The Baker Company, USA), according to the manufacturer's instructions.

Ubiquitination assays

Cells were lysed in a buffer containing 50 mM Tris-HCl (pH 7.5), 150 mM NaCl, 1% Nonidet P-40, and protease inhibitors. The obtained lysates were used for immunoprecipitation with anti-MKP-3 antibody followed by western blotting with an anti-ubiquitin antibody.

Western blot analysis

The harvested cells were lysed in RIPA lysis buffer (50 mM Tris-HCl [pH 7.5], 150 mM NaCl, 1% Nonidet P-40, 0.1% sodium dodecyl sulfate, and 0.5% sodium deoxycholate) supplemented with protease and phosphatase inhibitors on ice. For western blot analyses, aliquots with equal amounts of protein were loaded and separated by sodium dodecyl sul-

fate-polyacrylamide gel electrophoresis. Proteins were transferred onto nitrocellulose membranes (Bio-Rad, USA) and probed using specific antibodies, as indicated. The protein bands were visualized by chemiluminescence and detected using the ChemiDoc imaging system (Bio-Rad).

siRNA transfection

Predesigned siRNAs targeting human HIF-1α (#3091-1, #3091-2), MKP-3 (#1848-1), LDHA (#3939-1), ERK1 (#5595-1), ERK2 (#5594-1), and control siRNA (#SN-1001) were purchased from Bioneer (Korea). Transfections were performed using Lipofectamine™ RNAiMAX (Thermo Fisher Scientific), according to the manufacturer's instructions. One day after transfection, the cells were subjected to normoxia or hypoxia, as indicated. Protein knockdown was confirmed by western blot analysis.

MKP-3 overexpression

The human MKP-3 plasmid and empty vector were kindly provided by Dr. Tae Jun Park (Ajou University, Korea). Transient transfection of the plasmid into the RKO cells was performed using TurboFect™ Transfection Reagent (Thermo Fisher Scientific) according to the manufacturer's recommendations.

Cloning of DN-Erk1 (Erk1 K72R mutant)

The human Erk1 plasmid (hMU011474) was purchased from the Korea Human Gene Bank (Korea). A DNA fragment containing full-length human Erk1 coding sequences was subsequently subcloned into pCMV-Script (Stratagene, USA). To produce kinase-defective mutants of Erk1 (Chan et al., 2013), a lysine mutation in the pCMV-Script-ERK1 construct was generated using the QuikChange XL Directed Mutagenesis kit (Stratagene) and the following oligonucleotides: 5′-cgcgtggccatcaagaggatcagccccttcgaa-3′ and 5′-TTCGAAGGGGCTGATCCTCTTGATGGCCACGCG-3′ (Lys72 to Arg mutation).

RNA extraction and real-time reverse-transcription polymerase chain reaction (RT-qPCR)

Total RNA was isolated from the cells using the NucleoSpin RNA Plus Kit (MACHEREY-NAGEL, Germany) and reverse-transcribed using the iScript™ cDNA Synthesis Kit (Bio-Rad). The resulting cDNA was PCR-amplified with the appropriate primer pair: LDHA, 5′-GGATCTCCAACATGGCAGCCTT-3′ (forward) and 5′-AGACGGCTTTCTCCCTCTTGCT-3′ (reverse); VEGFA, 5′-TTGCCTTGCTGCTCTACCTCCA-3′ (forward) and 5′-GATGGCAGTAGCTGCGCTGATA-3′ (reverse); CA9, 5′-GTGCCTATGAGCAGTTGCTGTC-3′ (forward) and 5′-AAGTAGCGGCTGAAGTCAGAGG-3′ (reverse); GLUT1, 5′-TTGCAGGCTTCTCCAACTGGAC-3′ (forward) and 5′-CAGAACCAGGAGCACAGTGAAG-3′ (reverse); and 18S rRNA, 5′-AACCCGTTGAACCCCATT-3′ (forward) and 5′-CCATCCAATCGGTAGTAGCG-3′ (reverse) (Bioneer). RT-qPCR was performed with iQ SYBR™ Green Supermix (Bio-Rad) on a CFX Connect Real-Time PCR detection system (Bio-Rad). Gene-expression levels were determined using the comparative C_T ($\Delta\Delta C_T$) method and normalized to 18S ribosomal RNA.

Animals and syngeneic mouse tumor model

Seven male BALB/c mice (aged 5 weeks) were purchased from KOATECH (Korea) and allowed to acclimatize to their new environment for a week before beginning the experiment. For the syngeneic mouse tumor model, CT26 cells were harvested, washed twice in phosphate-buffered saline (PBS), and resuspended at a concentration of 1×10^7 cells/ml in PBS. CT26 cells (1×10^6 cells/100 μl/mouse) were injected subcutaneously into the right flank of the BALB/c mice. Tumor growth was assessed by measuring the tumor length and width using a caliper at 3- or 4-day intervals, and the tumor volume was calculated using the formula: volume = $0.523\ LW^2$ (L = length, W = width). All animal protocols adhered to the Ministry of Food and Drug Safety (MFDS) Guidelines for Care and Use of Laboratory Animals, and were approved by the Eulji University Laboratory Animal Care and Use Committee (approval No. EUIACUC18-29).

Immunofluorescence analysis of tissues

The tumors were fixed with 4% paraformaldehyde at 4°C overnight and then immersed in 30% sucrose/PBS for 48 h at 4°C. The tumors were immediately frozen in optimal cutting temperature compound (Tissue-Tek; Sakura Finetek USA, USA). The tumors were cut into 30 μm sections using a cryostat (Leica CM 1950; Leica, Germany). For immunofluorescence analysis of the tissues, the sections were blocked with 5% normal donkey serum (011-000-120; Jackson ImmunoResearch Laboratories, USA) for 1 h at room temperature (RT), followed by overnight incubation at 4°C with primary antibody against MKP-3 (ab76310; Abcam) or carbonic anhydrase IX/CA9 antibody (NB100-417; Novus Biologicals). The sections were then incubated with donkey anti-rabbit Alexa 488 (A-21206; Thermo Fisher Scientific) or donkey anti-rabbit Alexa 555 (A-31572; Thermo Fisher Scientific) for 1 h at RT. Thereafter, the sections were mounted in ProLong diamond Antifade mountant with DAPI (P36962; Invitrogen, USA). Finally, the slides were observed under an Eclipse E400 microscope (Nikon Instruments, USA), and images were captured using a Nikon Digital Sight DS-U2 camera.

Measurement of lactate

Conditioned media from normoxic and hypoxic cells were collected at the indicated time points to measure extracellular lactate levels. Conditioned media were filtered, and extracellular lactate was measured using the EZ-Lactate Assay kit (DoGenBio, Korea), according to the manufacturer's instructions.

Measurement of intracellular reactive oxygen species (ROS)

Intracellular ROS levels were measured using the cell-permeable fluorogenic probe H_2DCFDA (Thermo Fisher Scientific). Cells were placed in a hypoxia chamber (or retained under normoxic conditions for the control group) for 24 h. For the measurement of intracellular ROS, cells were incubated with 10 μM H_2DCFDA for 30 min at 37°C, harvested by trypsinization, and washed thrice with PBS. Fluorescence intensity was measured using a BD FACSMelody™ cell sorter (BD Life Sciences, USA). The background fluorescence was subtracted

from all samples.

Establishment of MKP-3 knockout (KO) clone

One day prior to transfection, CT26 cells were plated in 96-well plates at 10,000 cells/well. On the day of transfection, a master mix containing TrueCut Cas9 Protein v2 (Invitrogen) and MKP-3 gRNA (CRISPR247938_SGM; Invitrogen) was prepared in Opti-MEM medium (Invitrogen) and incubated for 5 min at RT to form the Cas9 RNPs. The Cas9 RNPs were added to the transfection reagent, CRISPRMAX™ (Invitrogen), diluted in Opti-MEM medium. The mixture was incubated at RT for 10 min to form the Cas9 RNA-transfection reagent complexes and then added to the cells. After incubation for two days, single cell clones were isolated by limiting dilution in 96 well plates. All single-cell clones were cultured, and KO was verified using western blot analysis. The validated KO single-cell clones were isolated, expanded, and used for further experiments.

Wound-healing assay

The CT26 cells were cultured in 6-well plates and grown to 100% confluence. The cell monolayer was scratched using a sterile 200 μl pipette tip. The plates were washed with PBS to remove detached cells and then incubated for 24 h. Cell migration was monitored, and live images were captured using the Juli stage (NanoEnTek, Korea) at 0 h and 24 h post-injury induction. The pixel count of the area of cell migration was obtained using ImageJ software (National Institutes of Health, USA).

Colony-formation assay

The CT26 cells were plated in six-well plates (1,000 cells/well) and allowed to grow for 7 days. Cells were washed with PBS, fixed in 4% formaldehyde for 15 min at RT, washed with PBS again, and stained with 0.1% crystal violet. Pictures were taken using a digital camera, and colony numbers were assessed visually.

Transwell migration assay

Chemotaxis was assayed using a Transwell migration assay. A total of 1×10^5 cells suspended in serum-free DMEM were added to the upper chambers (6.5 mm Transwell with 8.0 μm pore polycarbonate membrane insert; Corning, USA), and DMEM supplemented with 10% fetal bovine serum was added to the lower chambers as a chemoattractant. After incubation for 24 h at 37°C, the cells remaining on the upper surface of the membrane were removed, and the cells that had migrated to the underside of the membrane were fixed with 4% formaldehyde and stained with 0.1% crystal violet. The migrated cells on the underside of the membrane were observed under a light microscope.

Immunofluorescence assay

RKO cells were fixed with 4% paraformaldehyde in PBS (pH 7.4) for 20 min at RT and permeabilized with 0.1% Triton X-100. Nonspecific binding was blocked with 5% normal goat serum for 1 h. Cells were then incubated overnight with HIF-1α antibody at 4°C, followed by incubation with Alexa Fluor 488-conjugated goat anti-rabbit IgG (A-11034; Thermo Fisher Scientific) for 1 h at RT. Nuclei were stained with Hoechst 33258. The locations of HIF-1α and nuclei were determined using a fluorescence microscope (EVOS FL Cell Imaging System; Thermo Fisher Scientific). Results were expressed as the mean fluorescence intensity of HIF-1α from three randomly chosen high-power (×20) fields in each well. Each assay was performed in triplicate.

Statistical analysis

Statistical analyses were performed using SigmaPlot software for Windows (ver. 12.5; Systat Software, USA). Quantitative data are expressed as the mean± SEM of at least three independent experiments. Significant differences were determined using the Student's *t*-test or ANOVA. Statistical significance was set at $P < 0.05$.

RESULTS

Hypoxia increased the MKP-3 protein level in an HIF-1α -dependent manner

Previous studies using different cell models, including endothelial cells and neurons, showed that MKP-3 levels were upregulated under hypoxic conditions (Manalo et al., 2005; Mishra and Delivoria-Papadopoulos, 2004). Therefore, we first examined whether we could replicate this finding in colon cancer cells. Western blot analyses confirmed that the MKP-3 level increased two-fold in hypoxic RKO cells compared to the MKP-3 level in normoxic RKO cells (Figs. 1A and 1B). Next, we used RT-qPCR to determine whether exposure to hypoxia results in potent induction of MKP-3 mRNA. Consistent with a previous study (Bermudez et al., 2011), MKP-3 mRNA was significantly induced in response to hypoxia in a time-dependent manner (Supplementary Fig. S1). In addition, pretreatment with actinomycin D, which is widely used as a transcription inhibitor, markedly hampered MKP-3 induction in hypoxic RKO cells (Supplementary Fig. S2). These data indicated that hypoxia enhances MKP-3 transcription.

Since Bermudez et al. (2011) demonstrated that hypoxia induces an HIF-1α–dependent increase in the MKP-3 mRNA levels in cancer cells, we knocked down HIF-1α using siRNAs. As shown in Figs. 1C and 1D, HIF-1α knockdown inhibited hypoxic induction of MKP-3 protein. We also performed knockdown experiments using other HIF-1α siRNA sequences (Supplementary Fig. S3, siHIF#2); additionally, we confirmed that MKP-3 induction is HIF-1α-dependent under hypoxic conditions. HIF-1α has been demonstrated to be regulated through phosphorylation by various kinases. Several studies have shown that MAPK-mediated HIF-1α phosphorylation is required for the stabilization and activation of transcriptional activity during hypoxia (Comerford et al., 2004; Minet et al., 2001; Sodhi et al., 2001). As anticipated, we found that pharmacological inhibition of MAPK activity downregulates HIF-1α in hypoxic colon cancer cells (Figs. 1E-1H). In hypoxic RKO cells, only PD98059, a specific inhibitor of the Erk1/2 signaling pathway, decreased HIF-1α induction in a dose-dependent manner (Fig. 1E, Supplementary Fig. S4). However, inhibitors of all three major MAPK subfamilies decreased HIF-1α induction in hypoxic HCT 116 and DLD-1 cells (Figs. 1F and 1G). It was consequently inferred that the Erk1/2 sig-

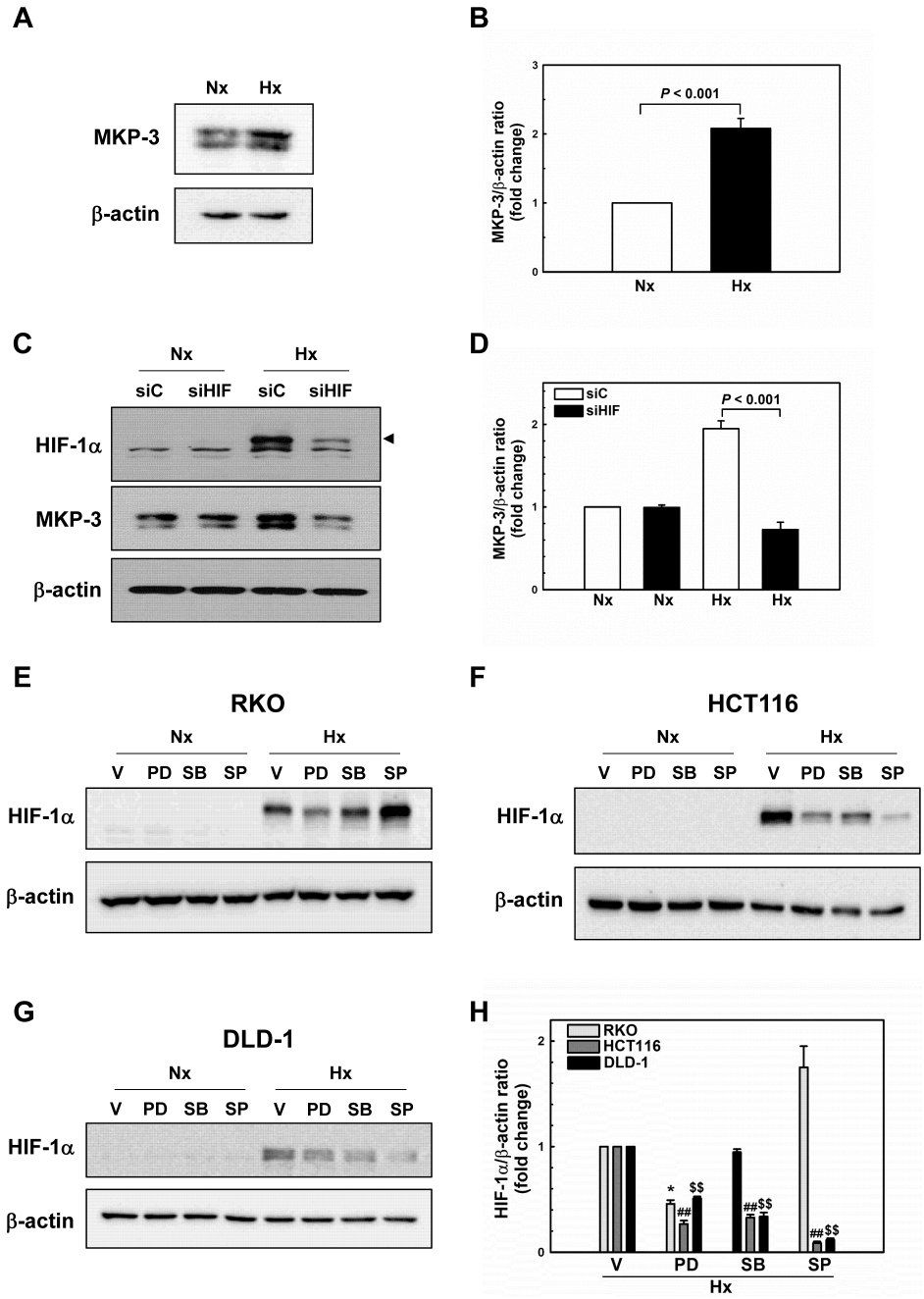

Fig. 1. Hypoxia increases MKP-3 protein level in an HIF-1α-dependent manner. (A and B) RKO cells were exposed to normoxic (Nx, 20% O_2) or hypoxic (Hx, 0.5% O_2) conditions for 6 h. MKP-3 protein level was analyzed by western blot analysis. (C and D) The RKO cells were transfected with either non-targeting siRNA (siC) or siRNA directed against HIF-1α (siHIF) for 48 h, and subsequently exposed to normoxia (Nx) or hypoxia (Hx) for 6 h. HIF-1α and MKP-3 levels were assessed by western blot analysis. RKO (E), HCT116 (F), and DLD-1 (G) cells were pretreated with MAPK inhibitors (20 μM PD98059 [PD], 10 μM SB203580 [SB], 10 μM SP600125 [SP]) or vehicle (V) for 1 h, and then exposed to normoxia (Nx) or hypoxia (Hx) for 6 h. HIF-1α protein level was assessed by western blot analysis. Representative western blots are shown. (H) Quantification of the HIF-1α/β-actin ratio. $^{*}P < 0.05$ vs RKO vehicle (V) control. $^{\#\#}P < 0.01$ vs HCT116 vehicle (V) control. $^{\$\$}P < 0.01$ vs DLD-1 vehicle (V) control. Results are presented as mean ± SEM of three independent experiments.

naling pathway routinely involves HIF-1α induction in hypoxic colon cancer cells. Since MKP-3 is well established as a cytoplasmic MKP specific for Erk1/2, which is required for HIF-1α stabilization and transcriptional activity (Richard et al., 1999), these results implied that hypoxia-induced MKP-3 may serve as a negative feedback regulator of HIF-1α.

Hypoxia-induced MKP-3 negatively regulated HIF-1α

To examine whether MKP-3 is a negative feedback regulator that controls the stability and transcriptional activity of HIF-1α, we used two approaches. First, we knocked down MKP-3 in colon cancer cells using siRNA and observed its effect on HIF-1α expression. Second, we overexpressed MKP-3 in colon cancer cells and evaluated its effect on HIF-1α expression.

As shown in Fig. 2A, the RKO cells transfected with MKP-3 siRNA showed markedly increased HIF-1α protein levels in a dose-dependent manner; however, control siRNA produced no effect on HIF-1α protein levels (Supplementary Fig. S5). Interestingly, HIF-2α protein levels remained unaffected (Fig. 2A). Moreover, these cells also showed significantly increased mRNA expression of *LDHA, VEGF, CA9,* and *GLUT1*; these are HIF-1α-dependent hypoxia-responsive genes, compared to the corresponding gene-expression profile in RKO cells

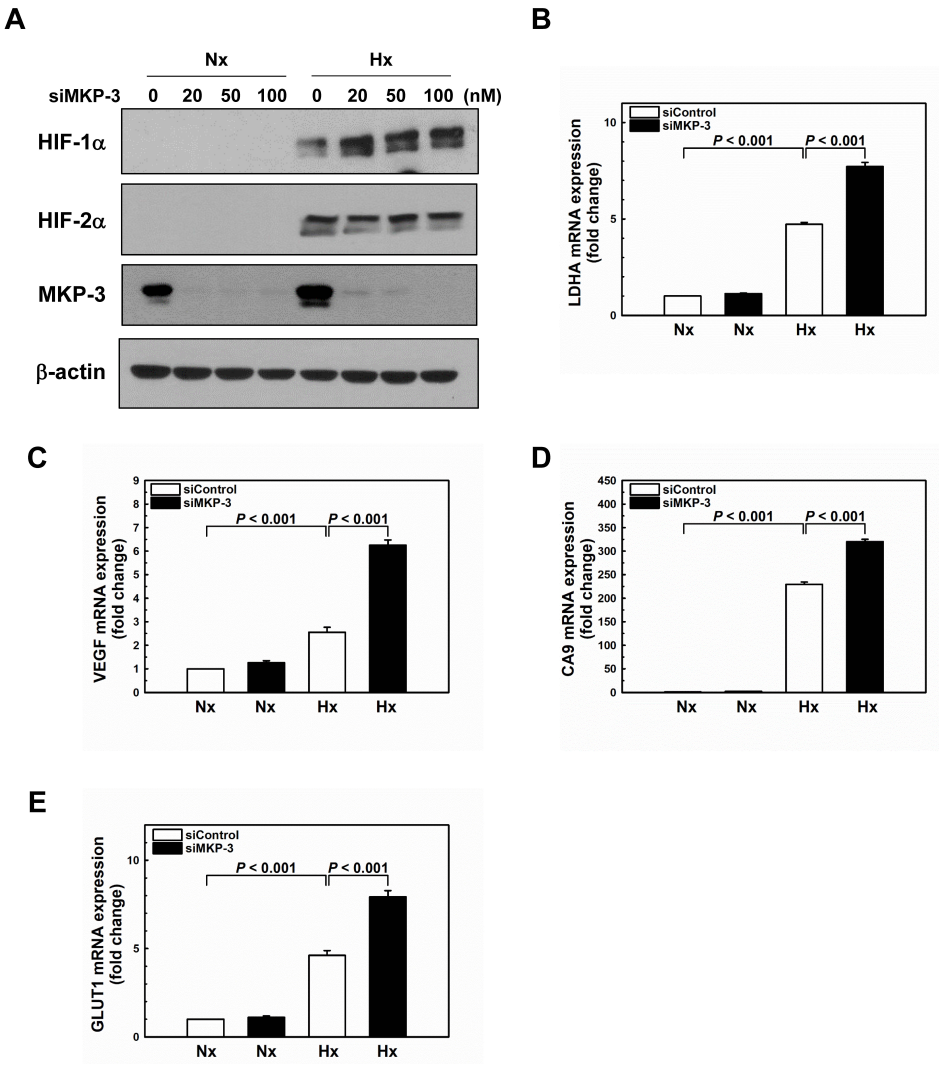

Fig. 2. Loss of MKP-3 increases HIF-1α protein level and its transcriptional activity in hypoxic colon cancer cells. (A) RKO cells were transfected with the indicated concentrations of MKP-3 siRNA constructs (0-100 nM) for 48 h, and then exposed to normoxia (Nx, 20% O_2) or hypoxia (Hx, 0.5% O_2) for 6 h. Western blot analysis was used to detect HIF-1α, HIF-2α, and MKP-3. β-Actin served as a loading control. A representative blot is shown (n = 3). RKO cells were transfected with either non-targeting siRNA (siControl) or siRNA directed against MKP-3 (siMKP-3) for 48 h, and then were exposed to normoxia (Nx) or hypoxia (Hx) for 24 h. mRNA levels of LDHA (B), VEGF (C), CA9 (D), and GLUT1 (E) were determined using quantitative RT-PCR. Results are shown as the mean ± SEM of 3-5 independent experiments.

transfected with control siRNA (Figs. 2B-2E).

We then evaluated the effect of MKP-3 overexpression on HIF-1α expression in RKO cells by transfecting the cells with a human MKP-3 plasmid. MKP-3 overexpression induced the dephosphorylation of Erk1/2, indicating the prevalent active state of exogenous MKP-3 (Fig. 3A). MKP-3 overexpression significantly decreased the HIF-1α protein (Figs. 3A and 3B), as well as HIF-1α-dependent hypoxia-responsive gene-expression, levels compared to the corresponding parameters in control vector-expressing RKO cells (Figs. 3C-3F); however, the HIF-2α level remained unimpacted (Fig. 3A).

Taken together, these data indicated that MKP-3 is a negative feedback effector that represses HIF-1α protein levels and expression of HIF-1α-dependent hypoxia-responsive genes.

Long-term hypoxia induced proteasomal degradation of MKP-3

Based on conventional categorization common in research and medical oncology, hypoxia may exist in two main forms in human tumors: chronic or acute (Hockel and Vaupel, 2001; Vaupel et al., 2001). Rapid tumor expansion leads to the development of long-term or chronic hypoxia in tumor tissues at distances greater than 70-150 μm from the patent blood vessels receiving insufficient oxygen. Therefore, we sought to determine whether long-term hypoxia affects MKP-3 expression levels. Results of time-course experiments revealed that MKP-3 protein levels peaked around 4 h and continuously decreased thereafter; additionally, they were undetectable around 24 h in colon cancer cells (Fig. 4A, Supplementary Fig. S6). Since MKP-3 is degraded by the ubiquitin–proteasome system (Marchetti et al., 2005), we tested the hypothesis that the reduced MKP-3 expression levels in colon cancer cells exposed to long-term hypoxia may be due to its accelerated degradation. These results (Fig. 4B, Supplementary Fig. S7) revealed that pretreatment with the proteasome inhibitor MG132 markedly prevents MKP-3 degradation caused by long-term hypoxia. We further showed that MKP-3 is efficiently ubiquitinated in response to long-term hypoxia (Supplementary Fig. S8). In addition, MKP-3 accumulation was observed following MG132 treatment under normoxic conditions, implying that MKP-3 may be constantly degraded via the proteasome in the resting state (Supple-

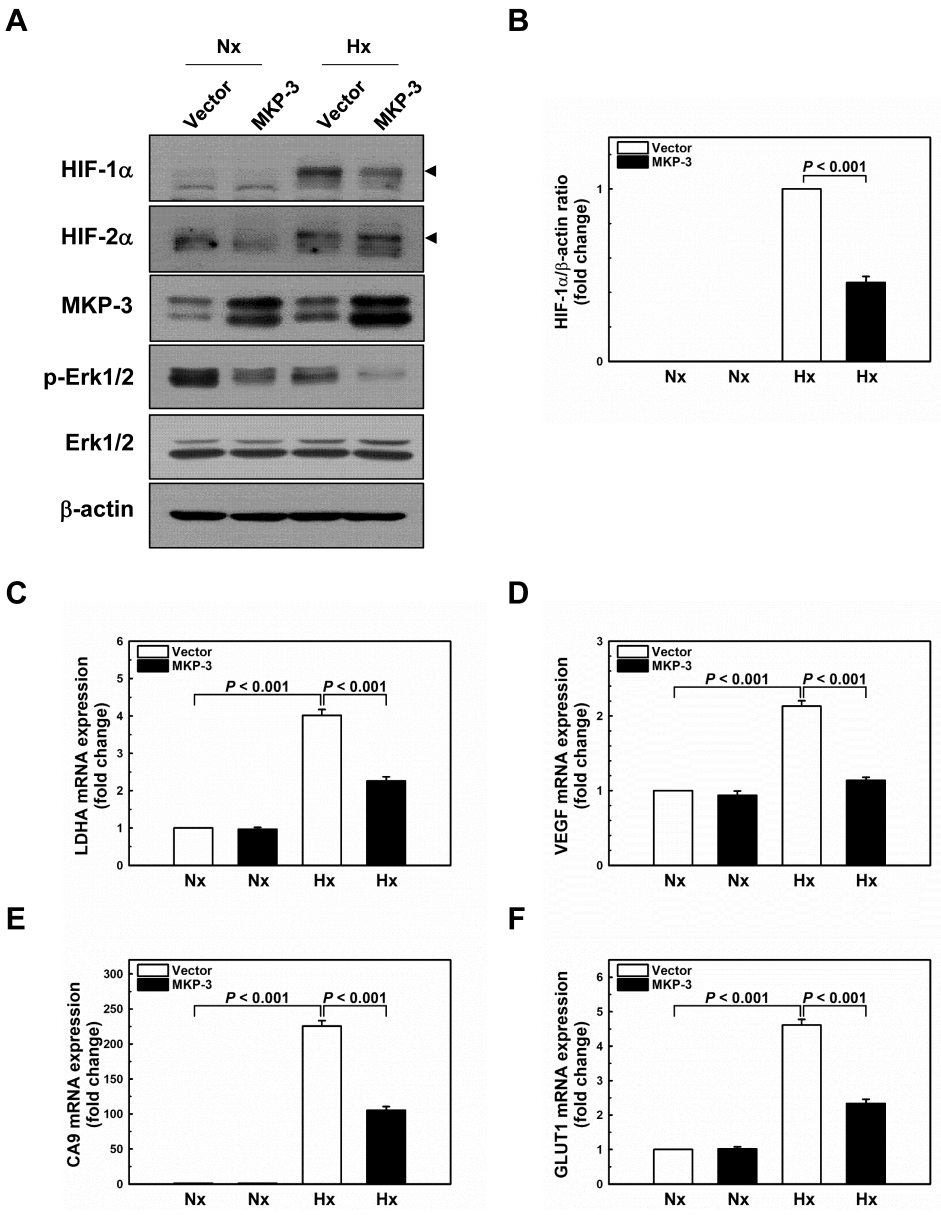

Fig. 3. MKP-3 overexpression decreases HIF-1α protein level and its transcriptional activity in hypoxic colon cancer cells. (A and B) RKO cells were transiently transfected either with empty vector (Vector) or human MKP-3 expression plasmid (MKP-3) for 24 h, and subsequently exposed to normoxia (Nx) or hypoxia (Hx) for 6 h. HIF-1α, HIF-2α, MKP-3, p-Erk1/2, total Erk1/2, and β-actin levels were assessed by western blot analysis. Arrowheads indicate HIF-1α or HIF-2α. RKO cells were transfected with either the empty vector or human MKP-3 expression plasmid for 24 h, and then exposed to normoxia (Nx) or hypoxia (Hx) for 24 h. mRNA level of LDHA (C), VEGF (D), CA9 (E), and GLUT1 (F) were determined by quantitative RT-PCR. Results are shown as the mean ± SEM of 3-5 independent experiments.

mentary Fig. S9). The *in vitro* results were recapitulated using an *in vivo* study (Supplementary Fig. S10), as allograft data also showed that MKP-3 is expressed throughout the tumor tissue; however, the staining was absent in the inner hypoxic area (Fig. 4C). It has been proposed that CA9 expression can be used as a surrogate marker for tumor hypoxia (Beasley et al., 2001). Therefore, we examined the expression of MKP-3 in relation to that of CA9. The distribution patterns of the two proteins did not overlap in the cells. CA9 expression was absent in the outer well-oxygenated areas but was present at a significantly higher level in the inner hypoxic areas (Supplementary Fig. S11). Thus, the reduction in the level of the MKP-3 protein caused by long-term hypoxia observed in cell culture appeared to be reflected in the striking focal patterns of expression around the inner hypoxic areas.

High levels of lactate, the end-product of anaerobic glucose catabolism, have been associated with poor clinical outcomes in several types of human cancers, and directly contribute to tumor growth and progression (Dhup et al., 2012). To investigate whether hypoxia induces the production of lactate in colon cancer cells, we examined lactate dehydrogenase A (LDHA) protein levels and measured lactate secretion by colon cancer cells following culture under normoxia or hypoxia for 24 h. The LDHA protein levels peaked around 8 h and were sustained for 24 h in hypoxic RKO cells (Fig. 5A). Consistent with this, RKO cells secreted significantly higher levels of lactate (4.3-fold higher) under hypoxia than under normoxia (Fig. 5B). Similarly, HCT116 cells also exhibited 1.8-fold enhanced production and secretion of lactate under hypoxic conditions compared to the corresponding production and secretion seen under normoxic conditions (Fig. 5C).

We then examined whether lactic acid influences MKP-3

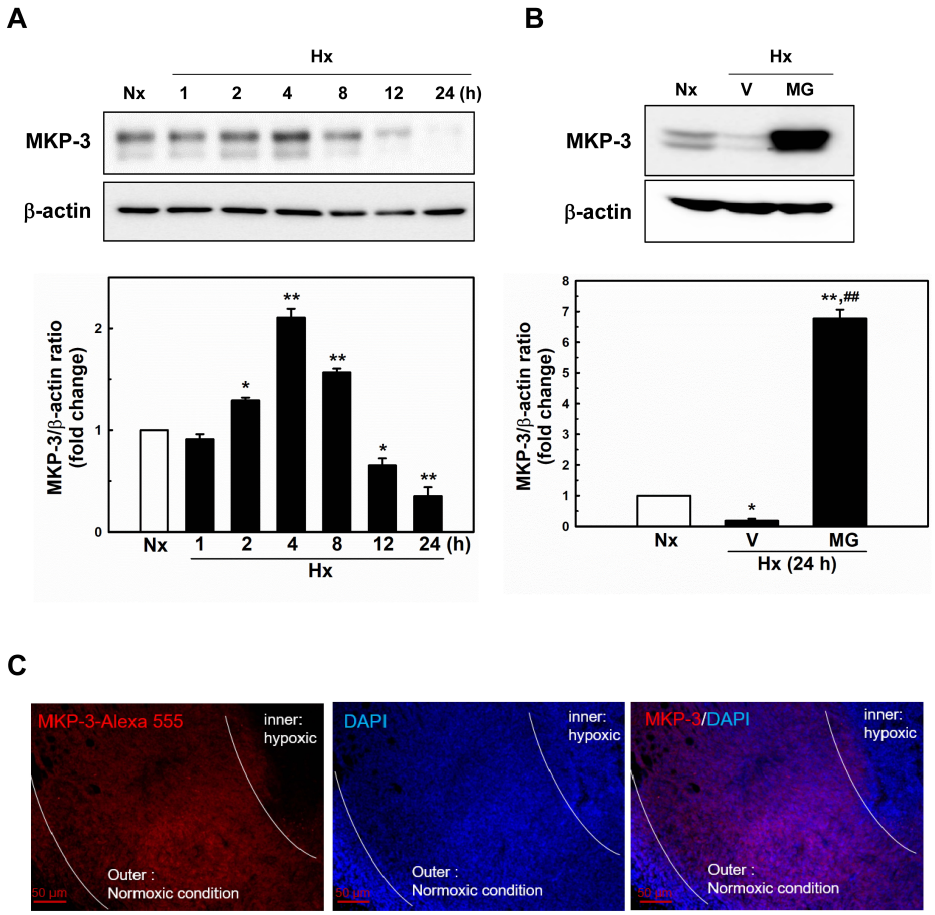

Fig. 4. Long-term hypoxia induces MKP-3 proteasomal degradation. (A) RKO cells were exposed to normoxia (Nx, 20% O_2) or hypoxia (Hx, 0.5% O_2) for the indicated time periods (1-24 h); MKP-3 and β-actin levels were assessed by western blot analysis. (B) RKO cells were pretreated with vehicle (V) or 10 mM MG132 (MG) for 1 h. Thereafter, the cells were exposed to normoxia (Nx) or hypoxia (Hx) for 24 h, and MKP-3 and β-actin levels were examined by western blot analysis. Representative western blots are shown (n = 3). $*P < 0.05$, $**P < 0.01$ vs normoxia control. $^{\#\#}P < 0.01$ vs hypoxia vehicle (V) control. (C) Representative immunofluorescence images of CT26 tumor sections stained for MKP-3. The nuclei are stained blue (DAPI) and the localization of MKP-3 visualized in red (Alexa 555). Scale bars = 50 μm.

protein levels. As shown in Fig. 6A and Supplementary Fig. S12, lactic acid treatment reduced the MKP-3 protein levels in colon cancer cells. MG132 pretreatment protected MKP-3 from lactic acid degradation (Supplementary Fig. S13), indicating that lactic acid can induce proteasomal degradation of MKP-3. To further ascertain the role of lactic acid in promoting MKP-3 degradation, we knocked down LDHA using siRNAs. The results showed that LDHA knockdown markedly attenuated MKP-3 degradation induced by long-term hypoxia in RKO cells (Fig. 6B). Similarly, pretreatment of colorectal cancer cells with sodium oxamate, an LDH inhibitor, restored the MKP-3 protein levels (Supplementary Fig. S14). Since lactate has been shown to activate Erk1/2 (Mu et al., 2018), which promotes MKP-3 proteasomal degradation (Marchetti et al., 2005), we examined whether lactic acid induces MKP-3 degradation via Erk1/2 activation. Exposure of RKO cells to lactic acid significantly activated Erk1/2 (Fig. 6C), and long-term hypoxia also induced Erk1/2 activation (Fig. 6D). To establish whether the Erk1/2 pathway is required for the proteasomal degradation of MKP-3 in response to lactic acid, RKO cells were transfected with Erk1/2 siRNAs or the dominant–negative form of Erk1 (DN-Erk1). Surprisingly, however, both Erk1/2 knockdown and DN-Erk1 overexpression failed to generate a protective effect on lactic acid-induced MKP-3 degradation, and even reduced basal MKP-3 levels (Supplementary Fig. S15). It was consequently inferred that Erk1/2 is an important regulator of MKP-3 in both a positive feed-forward and negative feedback loop. These findings are further supported by a previous study that MKP-3 mRNA synthesis is Erk1/2-dependent (Jurek et al., 2009).

Previous studies have also shown that the inactivation and degradation of MKP-3 are mediated by ROS (Chan et al., 2008), which are believed to be induced by hypoxia (Azimi et al., 2017). To test whether ROS are involved in the proteasomal degradation of MKP-3, cells were pretreated with the antioxidant N-acetylcysteine (NAC) and exposed to either normoxia or hypoxia. As shown in Supplementary Figs. S16A and S16B, NAC produced no effect on MKP-3 degradation under long-term hypoxic conditions. Moreover, exposure of RKO cells to long-term hypoxia also resulted in a minor decrease in intracellular ROS levels, as measured by dichlorofluorescein (DCF) fluorescence (Supplementary Fig. S16C). These results indicated that long-term hypoxia-induced proteasomal degradation of MKP-3 is mediated by lactic acid and not by ROS.

Loss of MKP-3 promoted cell proliferation and motility

Previous studies have indicated that MKP-3 acts as a tumor suppressor in several types of tumors (Chan et al., 2008; Furukawa et al., 2003; Ma et al., 2013). Moreover, Beaudry et al. (2019) recently reported that MKP-3 gene deletion markedly enhanced the tumor load in $Apc^{Min/+}$ mice. Therefore, we

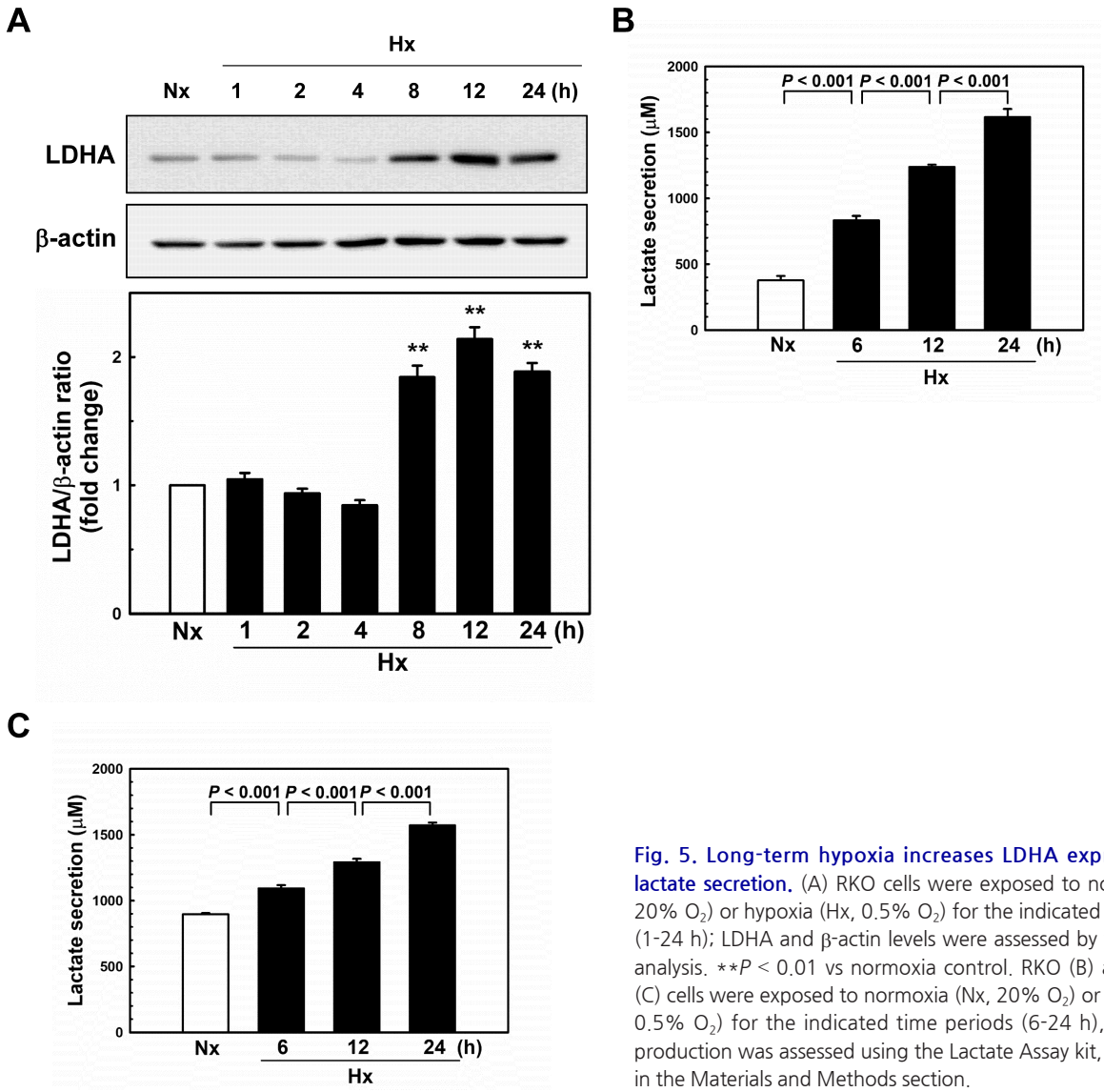

Fig. 5. Long-term hypoxia increases LDHA expression and lactate secretion. (A) RKO cells were exposed to normoxia (Nx, 20% O_2) or hypoxia (Hx, 0.5% O_2) for the indicated time periods (1-24 h); LDHA and β-actin levels were assessed by western blot analysis. $^{**}P < 0.01$ vs normoxia control. RKO (B) and HCT116 (C) cells were exposed to normoxia (Nx, 20% O_2) or hypoxia (Hx, 0.5% O_2) for the indicated time periods (6-24 h), and lactate production was assessed using the Lactate Assay kit, as described in the Materials and Methods section.

generated MKP-3 KO clones in CT26 cells using CRISPR/Cas9 technology to determine the role of MKP-3 in the tumorigenic phenotype of colon cancer cells *in vitro* (Fig. 7A). MKP-3 KO cells showed a marked increase in colony-formation ability compared to that seen in wild-type (WT) cells (Fig. 7B). Cell migration was analyzed using wound-healing and Transwell migration assays. As shown in Figs. 7C and 7D, the loss of MKP-3 significantly increased cell motility. MKP-3 KO CT26 cells also showed a robust migratory phenotype in the Transwell migration assay (Supplementary Fig. S17). In addition, we observed that MKP-3 KO cells showed a marked increase in HIF-1α induction (Supplementary Fig. S18) and accelerated cell motility (Supplementary Figs. S19 and S20) compared with the corresponding parameters in WT cells. These results are concordant with previous findings, in which the loss of MKP-3 was found to enhance the tumorigenic potential of colon cancer cells.

DISCUSSION

MKP-3 has been proposed as a novel candidate tumor suppressor in several tumor types, including esophageal squamous cell carcinoma, non-small cell lung cancer, ovarian cancer, and pancreatic cancer (Chan et al., 2008; Furukawa et al., 2003; Ma et al., 2013; Moncho-Amor et al., 2019). The MKP-3 expression has also been associated with cancer progression in myeloma, melanoma, glioma, and breast cancer (Bloethner et al., 2005; Croonquist et al., 2003; Ramnarain et al., 2006; Warmka et al., 2004). While MKP-3 is known to play a critical role in cancer progression, its regulation under hypoxic tumor conditions is not fully understood. A few studies have shown that hypoxia increases the endogenous levels of MKP-3 (Bermudez et al., 2011; Mishra and Delivoria-Papadopoulos, 2004). However, these studies did not address the role of MKP-3 under hypoxic conditions. In the present study, our results highlighted the pivotal role of MKP-3 in modu-

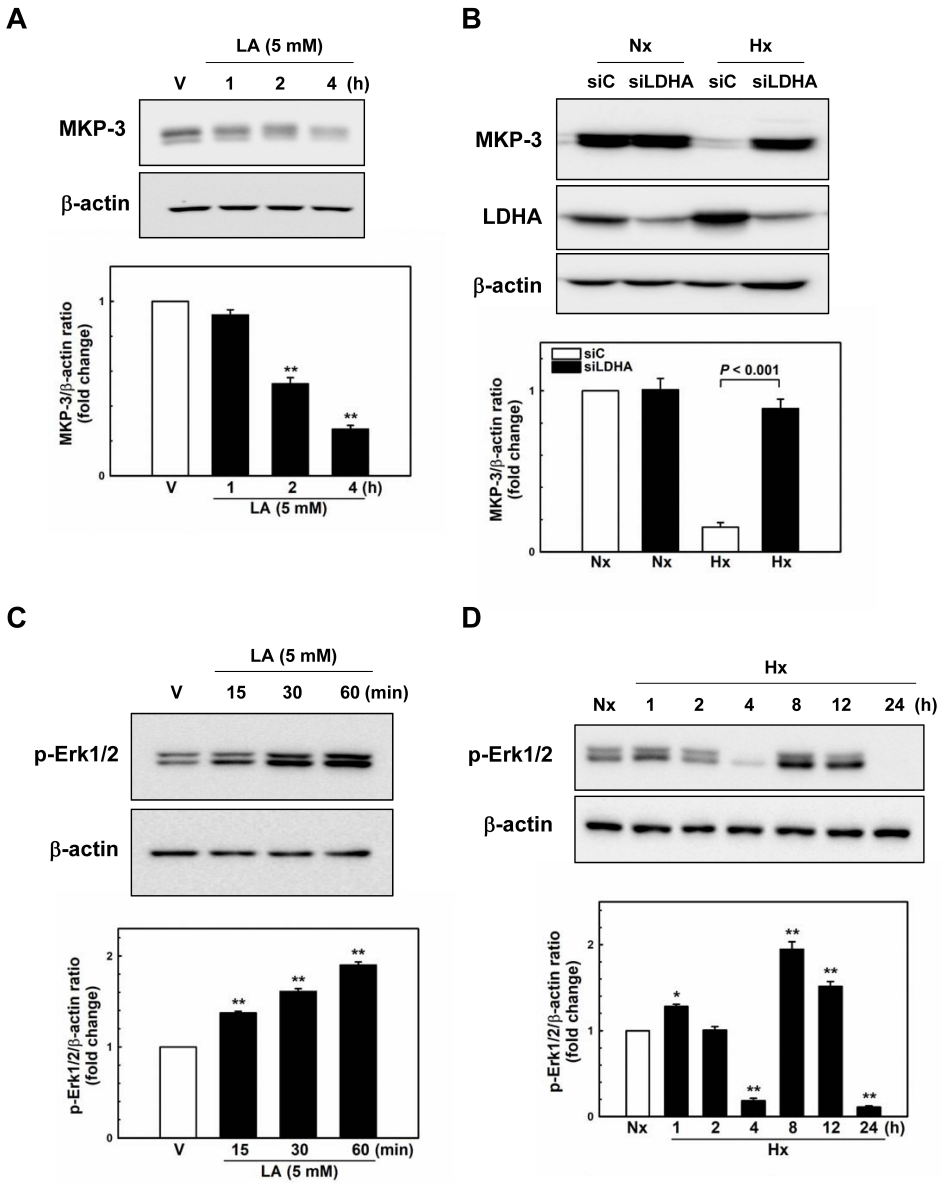

Fig. 6. Hypoxia-induced lactate promotes MKP-3 degradation through Erk1/2 activation. (A) RKO cells were treated with 5 mM lactic acid (LA) for the indicated time (0-4 h) periods; MKP-3 and β-actin levels were examined by western blot analysis. V, vehicle. (B) RKO cells were transfected with either non-targeting siRNA (siC) or siRNA directed against LDHA (siLDHA) for 48 h, and subsequently exposed to normoxia (Nx) or hypoxia (Hx) for 24 h. MKP-3, LDHA, and β-actin levels were assessed by western blot analysis. (C) RKO cells were treated with 5 mM lactic acid (LA) for the indicated time periods (15-60 min), and Erk1/2 activation was assessed by western blot analysis. (D) RKO cells were exposed to normoxia (Nx, 20% O_2) or hypoxia (Hx, 0.5% O_2) for the indicated time periods (1-24 h), and p-Erk1/2 and β-actin levels were assessed by western blot analysis. $*P < 0.05$, $**P < 0.01$ vs vehicle or normoxia control. Representative western blots are shown (n = 3).

lating HIF-1α protein levels, and further showed that MKP-3 negatively regulates HIF-1α-dependent gene expression in hypoxia-exposed human colon cancer cells (Figs. 2 and 3). In three different human colon cancer cell lines, our data showed that MAPKs are involved in regulating HIF-1α protein levels (Figs. 1E-1H); however, only the Erk1/2 pathway is associated with HIF-1α induction in hypoxic RKO cells. Since MKP-3 is known to inactivate p38, JNK, and Erk1/2 (Arkell et al., 2008; Hsu et al., 2018), MKP-3 appears to modulate HIF-1α levels through the regulation of MAPKs. In the present study, it is unclear whether HIF-1α interacts with, or itself serves as, an MKP-3 substrate. However, the immunofluorescence assay revealed that MKP-3 overexpression failed to impact the nuclear localization of HIF-1α but decreased its fluorescence intensity (Supplementary Fig. S21). These data indicated that MKP-3 regulates HIF-1α protein levels but not its nuclear translocation.

HIF-2α is another transcription factor that is regulated by oxygen, similar to HIF-1α, and both activate hypoxia response element-dependent gene transcription (Koh and Powis, 2012). However, HIF-2α induction was not influenced by MKP-3 (Figs. 2A and 3A). Interestingly, Gkotinakou et al. (2019) recently reported that Erk1/2-mediated phosphorylation of HIF-2α regulates transcriptional activity and nuclear translocation without altering its protein-expression levels. Thus, MKP-3 may produce no inhibitory effect on HIF-2α protein levels, although HIF-1α and HIF-2α share 48% amino acid sequence identity and similar protein structures (Koh and Powis, 2012).

Surprisingly, we found that long-term hypoxia decreases the MKP-3 protein levels (Fig. 4A, Supplementary Fig. S6), and this was restored by proteasome inhibitor treatment (Fig. 4B, Supplementary Fig. S7); however, MKP-3 transcription was markedly enhanced (Supplementary Fig. S1).

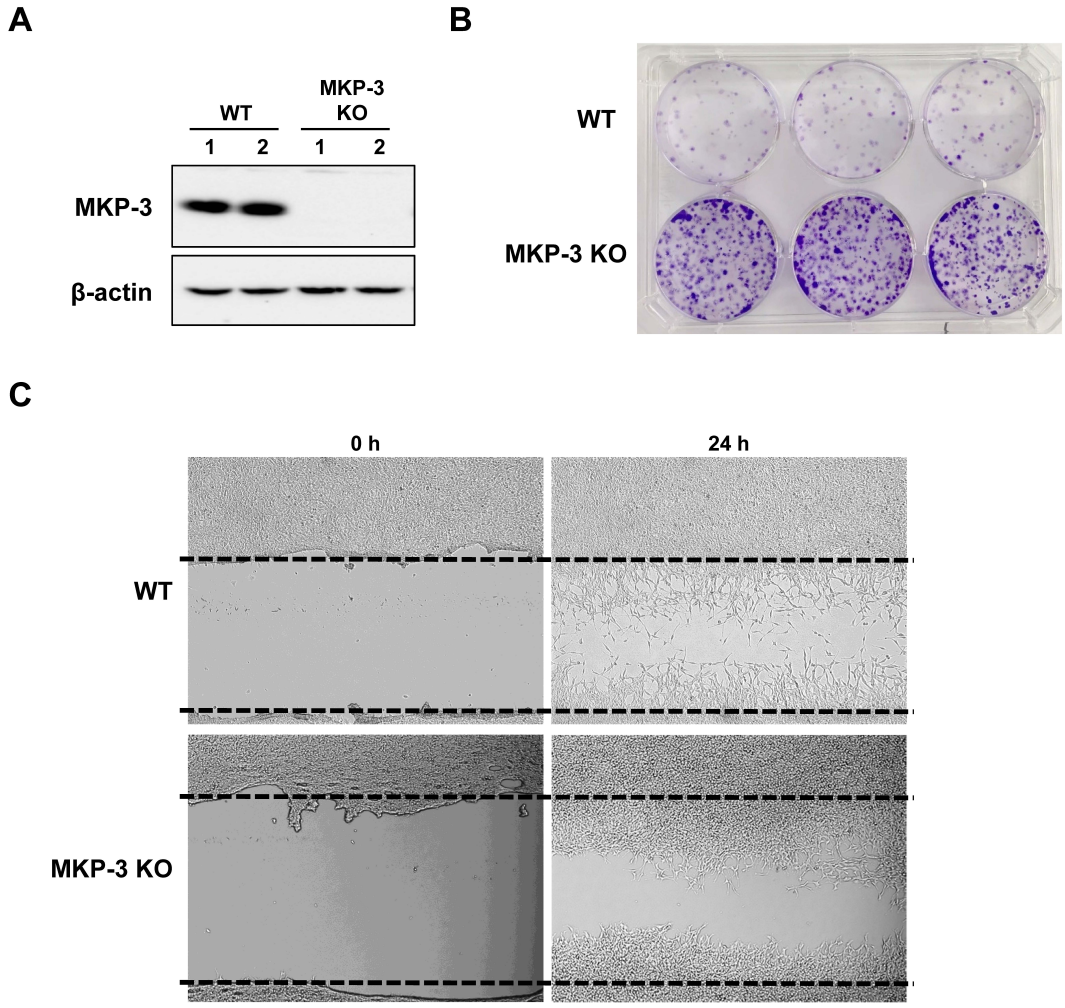

Fig. 7. Loss of MKP-3 promotes cell proliferation and motility. (A) Western blot analysis confirmed the loss of MKP-3 protein expression in MKP-3 KO CT26 mouse colon cancer cells, which were obtained using the CRISPR/Cas9 technology. β-Actin was used as a loading control. (B) Colony-formation assays showing crystal violet staining in the WT group and MKP-3 KO group. Representative results of colony-formation assays of three independent experiments. (C and D) CT26 cell motility was determined by measuring wound closure in the wound-healing assay using ImageJ software (magnification ×10). Results are shown as the mean ± SEM of three independent experiments.

These results implied that long-term hypoxia decreases the MKP-3 protein level by proteasomal degradation rather than transcriptional suppression. Tumor hypoxia directly increases lactate production and excretion; moreover, lactate levels in tumors can reach up to 40 mM, with an average level of 10 mM (Walenta and Mueller-Klieser, 2004). Consistent with earlier studies, a significant increase in lactate secretion was observed in RKO and HCT116 cells following long-term hypoxia (Figs. 5B and 5C), and knockdown of LDHA or LDH inhibitor protected MKP-3 from hypoxia-induced degradation (Fig. 6B, Supplementary Fig. S14). These data strongly indicated that long-term hypoxia-induced lactate promotes proteasomal degradation of MKP-3. Furthermore, exogenous lactic acid markedly activated Erk1/2 (Fig. 6C) and hypoxia also increased active Erk1/2 at later time points (>8 h) (Fig. 6D). This therefore indicated that lactate-induced Erk1/2

activation is involved in MKP-3 degradation under long-term hypoxia. After 24 h of hypoxia, Erk1/2 phosphorylation was suppressed completely (Fig. 6D); this was most likely attributable to negative feedback, which determines the duration and amplitude of Erk1/2 activation (Shin et al., 2009).

MKP-3 downregulation is attributed to epigenetic silencing, 12q21 allelic loss, and proteasomal degradation mediated by oxidative stress in cancer (Chan et al., 2008; Furukawa et al., 2003; Wong et al., 2012; Xu et al., 2005). To the best of our knowledge, the present study is the first to demonstrate that long-term hypoxia induces the loss of MKP-3 through lactate-mediated Erk1/2 activation in colon cancer cells.

Finally, because MKP-3 has been proposed as a tumor suppressor, we sought to determine whether the loss of MKP-3 induced by hypoxia affects the phenotypes of colon cancer cells. Consistent with the results of the study by Beaudry et al. (2019) involving $Apc^{Min/+}$ mice, MKP-3 KO CT26 mouse colon cancer cells showed increased proliferation and enhanced migration ability (Fig. 7). Additionally, inactivation of MKP-3 correlates with Erk2-dependent epithelial–mesenchymal transition (EMT) and contributes to colon cancer invasion (Li et al., 2014). Therefore, it is reasonable to speculate that the loss of MKP-3 in cancer cells from hypoxic regions may accelerate the processes that are essential for metastasis, such as EMT, migration, and invasion in colon cancer.

In summary, long-term hypoxia promotes proteasomal degradation of MKP-3, which has a suppressive role in HIF-1, α and the loss of MKP-3 is involved in changes in the proliferative and migratory phenotype of human colon cancer cells. Therefore, upregulation or maintenance of MKP-3 may serve as an efficacious therapeutic strategy to regulate hypoxia-induced changes in colon cancer cells and inhibit cancer cell proliferation and migration.

Note: Supplementary information is available on the Molecules and Cells website (www.molcells.org).

ACKNOWLEDGMENTS

The present study was supported by a grant to H.S.K. from the National Research Foundation of Korea (NRF) grants (NRF-2018R1D1A1B07040397).

AUTHOR CONTRIBUTIONS

H.S.K., M.S.L., and Y.H.K. conceived, performed experiments, and wrote the manuscript. J.L., S.R.H., D.B.K., H.K., and S.P. performed experiments.

CONFLICT OF INTEREST

The authors have no potential conflicts of interest to disclose.

ORCID

Hong Seok Kim https://orcid.org/0000-0001-7533-8979
Yun Hee Kang https://orcid.org/0000-0002-2490-6080
Jisu Lee https://orcid.org/0000-0001-7936-9860
Seung Ro Han https://orcid.org/0000-0002-5115-3045
Da Bin Kim https://orcid.org/0000-0002-9176-7340
Haeun Ko https://orcid.org/0000-0003-1278-1556
Seyoun Park https://orcid.org/0000-0003-4746-3785
Myung-Shin Lee https://orcid.org/0000-0001-9145-6190

REFERENCES

Arkell, R.S., Dickinson, R.J., Squires, M., Hayat, S., Keyse, S.M., and Cook, S.J. (2008). DUSP6/MKP-3 inactivates ERK1/2 but fails to bind and inactivate ERK5. Cell. Signal. *20*, 836-843.

Azimi, I., Petersen, R.M., Thompson, E.W., Roberts-Thomson, S.J., and Monteith, G.R. (2017). Hypoxia-induced reactive oxygen species mediate N-cadherin and SERPINE1 expression, EGFR signalling and motility in MDA-MB-468 breast cancer cells. Sci. Rep. *7*, 15140.

Beasley, N.J., Wykoff, C.C., Watson, P.H., Leek, R., Turley, H., Gatter, K., Pastorek, J., Cox, G.J., Ratcliffe, P., and Harris, A.L. (2001). Carbonic anhydrase IX, an endogenous hypoxia marker, expression in head and neck squamous cell carcinoma and its relationship to hypoxia, necrosis, and microvessel density. Cancer Res. *61*, 5262-5267.

Beaudry, K., Langlois, M.J., Montagne, A., Cagnol, S., Carrier, J.C., and Rivard, N. (2019). Dual-specificity phosphatase 6 deletion protects the colonic epithelium against inflammation and promotes both proliferation and tumorigenesis. J. Cell. Physiol. *234*, 6731-6745.

Bermudez, O., Jouandin, P., Rottier, J., Bourcier, C., Pages, G., and Gimond, C. (2011). Post-transcriptional regulation of the DUSP6/MKP-3 phosphatase by MEK/ERK signaling and hypoxia. J. Cell. Physiol. *226*, 276-284.

Bloethner, S., Chen, B., Hemminki, K., Muller-Berghaus, J., Ugurel, S., Schadendorf, D., and Kumar, R. (2005). Effect of common B-RAF and N-RAS mutations on global gene expression in melanoma cell lines. Carcinogenesis *26*, 1224-1232.

Byun, Y., Choi, Y.C., Jeong, Y., Yoon, J., and Baek, K. (2020). Long noncoding RNA expression profiling reveals upregulation of uroplakin 1A and uroplakin 1A antisense RNA 1 under hypoxic conditions in lung cancer cells. Mol. Cells *43*, 975-988.

Camps, M., Nichols, A., and Arkinstall, S. (2000). Dual specificity phosphatases: a gene family for control of MAP kinase function. FASEB J. *14*, 6-16.

Caunt, C.J. and Keyse, S.M. (2013). Dual-specificity MAP kinase phosphatases (MKPs): shaping the outcome of MAP kinase signalling. FEBS J. *280*, 489-504.

Chan, D.W., Liu, V.W., Tsao, G.S., Yao, K.M., Furukawa, T., Chan, K.K., and Ngan, H.Y. (2008). Loss of MKP3 mediated by oxidative stress enhances tumorigenicity and chemoresistance of ovarian cancer cells. Carcinogenesis *29*, 1742-1750.

Chan, G., Gu, S., and Neel, B.G. (2013). Erk1 and Erk2 are required for maintenance of hematopoietic stem cells and adult hematopoiesis. Blood *121*, 3594-3598.

Chang, L. and Karin, M. (2001). Mammalian MAP kinase signalling cascades. Nature *410*, 37-40.

Comerford, K.M., Cummins, E.P., and Taylor, C.T. (2004). c-Jun NH2-terminal kinase activation contributes to hypoxia-inducible factor 1alpha-dependent P-glycoprotein expression in hypoxia. Cancer Res. *64*, 9057-9061.

Croonquist, P.A., Linden, M.A., Zhao, F., and Van Ness, B.G. (2003). Gene profiling of a myeloma cell line reveals similarities and unique signatures among IL-6 response, N-ras-activating mutations, and coculture with bone marrow stromal cells. Blood *102*, 2581-2592.

Dhillon, A.S., Hagan, S., Rath, O., and Kolch, W. (2007). MAP kinase signalling pathways in cancer. Oncogene *26*, 3279-3290.

Dhup, S., Dadhich, R.K., Porporato, P.E., and Sonveaux, P. (2012). Multiple biological activities of lactic acid in cancer: influences on tumor growth, angiogenesis and metastasis. Curr. Pharm. Des. *18*, 1319-1330.

Furukawa, T., Sunamura, M., Motoi, F., Matsuno, S., and Horii, A. (2003). Potential tumor suppressive pathway involving DUSP6/MKP-3 in pancreatic cancer. Am. J. Pathol. *162*, 1807-1815.

Gkotinakou, I.M., Befani, C., Simos, G., and Liakos, P. (2019). ERK1/2 phosphorylates HIF-2alpha and regulates its activity by controlling its CRM1-dependent nuclear shuttling. J. Cell Sci. *132*, jcs225698.

Harris, A.L. (2002). Hypoxia--a key regulatory factor in tumour growth. Nat. Rev. Cancer *2*, 38-47.

Hockel, M. and Vaupel, P. (2001). Biological consequences of tumor hypoxia. Semin. Oncol. *28*(2 Suppl 8), 36-41.

Hsu, W.C., Chen, M.Y., Hsu, S.C., Huang, L.R., Kao, C.Y., Cheng, W.H., Pan, C.H., Wu, M.S., Yu, G.Y., Hung, M.S., et al. (2018). DUSP6 mediates T cell receptor-engaged glycolysis and restrains TFH cell differentiation. Proc. Natl. Acad. Sci. U. S. A. *115*, E8027-E8036.

Jurek, A., Amagasaki, K., Gembarska, A., Heldin, C.H., and Lennartsson, J. (2009). Negative and positive regulation of MAPK phosphatase 3 controls platelet-derived growth factor-induced Erk activation. J. Biol. Chem. *284*, 4626-4634.

Keyse, S.M. (2000). Protein phosphatases and the regulation of mitogen-activated protein kinase signalling. Curr. Opin. Cell Biol. *12*, 186-192.

Keyse, S.M. (2008). Dual-specificity MAP kinase phosphatases (MKPs) and cancer. Cancer Metastasis Rev. *27*, 253-261.

Kietzmann, T., Mennerich, D., and Dimova, E.Y. (2016). Hypoxia-inducible factors (HIFs) and phosphorylation: impact on stability, localization, and transactivity. Front. Cell Dev. Biol. *4*, 11.

Koh, M.Y. and Powis, G. (2012). Passing the baton: the HIF switch. Trends Biochem. Sci. *37*, 364-372.

Li, C., Ma, H., Wang, Y., Cao, Z., Graves-Deal, R., Powell, A.E., Starchenko, A., Ayers, G.D., Washington, M.K., Kamath, V., et al. (2014). Excess PLAC8 promotes an unconventional ERK2-dependent EMT in colon cancer. J. Clin. Invest. *124*, 2172-2187.

Ma, J., Yu, X., Guo, L., and Lu, S.H. (2013). DUSP*6*, a tumor suppressor, is involved in differentiation and apoptosis in esophageal squamous cell carcinoma. Oncol. Lett. *6*, 1624-1630.

Manalo, D.J., Rowan, A., Lavoie, T., Natarajan, L., Kelly, B.D., Ye, S.Q., Garcia, J.G., and Semenza, G.L. (2005). Transcriptional regulation of vascular endothelial cell responses to hypoxia by HIF-1. Blood *105*, 659-669.

Marchetti, S., Gimond, C., Chambard, J.C., Touboul, T., Roux, D., Pouyssegur, J., and Pages, G. (2005). Extracellular signal-regulated kinases phosphorylate mitogen-activated protein kinase phosphatase 3/DUSP6 at serines 159 and 197, two sites critical for its proteasomal degradation. Mol. Cell. Biol. *25*, 854-864.

Minet, E., Michel, G., Mottet, D., Raes, M., and Michiels, C. (2001). Transduction pathways involved in Hypoxia-Inducible Factor-1 phosphorylation and activation. Free Radic. Biol. Med. *31*, 847-855.

Mishra, O.P. and Delivoria-Papadopoulos, M. (2004). Effect of hypoxia on the expression and activity of mitogen-activated protein (MAP) kinase-phosphatase-1 (MKP-1) and MKP-3 in neuronal nuclei of newborn piglets: the role of nitric oxide. Neuroscience *129*, 665-673.

Moncho-Amor, V., Pintado-Berninches, L., Ibanez de Caceres, I., Martin-Villar, E., Quintanilla, M., Chakravarty, P., Cortes-Sempere, M., Fernandez-Varas, B., Rodriguez-Antolin, C., de Castro, J., et al. (2019). Role of Dusp6 phosphatase as a tumor suppressor in non-small cell lung cancer. Int. J. Mol. Sci. *20*, 2036.

Mu, X., Shi, W., Xu, Y., Xu, C., Zhao, T., Geng, B., Yang, J., Pan, J., Hu, S., Zhang, C., et al. (2018). Tumor-derived lactate induces M2 macrophage polarization via the activation of the ERK/STAT3 signaling pathway in breast cancer. Cell Cycle *17*, 428-438.

Olive, P.L., Vikse, C., and Trotter, M.J. (1992). Measurement of oxygen diffusion distance in tumor cubes using a fluorescent hypoxia probe. Int. J. Radiat. Oncol. Biol. Phys. *22*, 397-402.

Ramnarain, D.B., Park, S., Lee, D.Y., Hatanpaa, K.J., Scoggin, S.O., Otu, H., Libermann, T.A., Raisanen, J.M., Ashfaq, R., Wong, E.T., et al. (2006). Differential gene expression analysis reveals generation of an autocrine loop by a mutant epidermal growth factor receptor in glioma cells. Cancer Res. *66*, 867-874.

Rankin, E.B. and Giaccia, A.J. (2008). The role of hypoxia-inducible factors in tumorigenesis. Cell Death Differ. *15*, 678-685.

Richard, D.E., Berra, E., Gothie, E., Roux, D., and Pouyssegur, J. (1999). p42/p44 mitogen-activated protein kinases phosphorylate hypoxia-inducible factor 1alpha (HIF-1alpha) and enhance the transcriptional activity of HIF-1. J. Biol. Chem. *274*, 32631-32637.

Semenza, G.L. (2010). Defining the role of hypoxia-inducible factor 1 in cancer biology and therapeutics. Oncogene *29*, 625-634.

Semenza, G.L. (2012). Hypoxia-inducible factors in physiology and medicine. Cell *148*, 399-408.

Shen, Z., Zhang, C., Qu, L., Lu, C., Xiao, M., Ni, R., and Liu, J. (2019). MKP-4 suppresses hepatocarcinogenesis by targeting ERK1/2 pathway. Cancer Cell Int. *19*, 61.

Shin, S.Y., Rath, O., Choo, S.M., Fee, F., McFerran, B., Kolch, W., and Cho, K.H. (2009). Positive- and negative-feedback regulations coordinate the dynamic behavior of the Ras-Raf-MEK-ERK signal transduction pathway. J. Cell Sci. *122*, 425-435.

Sodhi, A., Montaner, S., Miyazaki, H., and Gutkind, J.S. (2001). MAPK and Akt act cooperatively but independently on hypoxia inducible factor-1alpha in rasV12 upregulation of VEGF. Biochem. Biophys. Res. Commun. *287*, 292-300.

Urosevic, J., Garcia-Albeniz, X., Planet, E., Real, S., Cespedes, M.V., Guiu, M., Fernandez, E., Bellmunt, A., Gawrzak, S., Pavlovic, M., et al. (2014). Colon cancer cells colonize the lung from established liver metastases through p38 MAPK signalling and PTHLH. Nat. Cell Biol. *16*, 685-694.

Vaupel, P., Thews, O., and Hoeckel, M. (2001). Treatment resistance of solid tumors: role of hypoxia and anemia. Med. Oncol. *18*, 243-259.

Wagner, E.F. and Nebreda, A.R. (2009). Signal integration by JNK and p38 MAPK pathways in cancer development. Nat. Rev. Cancer *9*, 537-549.

Waha, A., Felsberg, J., Hartmann, W., von dem Knesebeck, A., Mikeska, T., Joos, S., Wolter, M., Koch, A., Yan, P.S., Endl, E., et al. (2010). Epigenetic downregulation of mitogen-activated protein kinase phosphatase MKP-2 relieves its growth suppressive activity in glioma cells. Cancer Res. *70*, 1689-1699.

Walenta, S. and Mueller-Klieser, W.F. (2004). Lactate: mirror and motor of tumor malignancy. Semin. Radiat. Oncol. *14*, 267-274.

Warmka, J.K., Mauro, L.J., and Wattenberg, E.V. (2004). Mitogen-activated protein kinase phosphatase-3 is a tumor promoter target in initiated cells that express oncogenic Ras. J. Biol. Chem. *279*, 33085-33092.

Wenger, R.H., Stiehl, D.P., and Camenisch, G. (2005). Integration of oxygen signaling at the consensus HRE. Sci. STKE *2005*, re12.

Wong, V.C., Chen, H., Ko, J.M., Chan, K.W., Chan, Y.P., Law, S., Chua, D., Kwong, D.L., Lung, H.L., Srivastava, G., et al. (2012). Tumor suppressor dual-specificity phosphatase 6 (DUSP6) impairs cell invasion and epithelial-mesenchymal transition (EMT)-associated phenotype. Int. J. Cancer *130*, 83-95.

Xu, S., Furukawa, T., Kanai, N., Sunamura, M., and Horii, A. (2005). Abrogation of DUSP6 by hypermethylation in human pancreatic cancer. J. Hum. Genet. *50*, 159-167.

Zhu, M.M., Tong, J.L., Xu, Q., Nie, F., Xu, X.T., Xiao, S.D., and Ran, Z.H. (2012). Increased JNK1 signaling pathway is responsible for ABCG2-mediated multidrug resistance in human colon cancer. PLoS One *7*, e41763.